JOURNAL OF SOLID STATE CHEMISTRY **127,** 202–210 (1996)
ARTICLE NO. 0376

Contributions to the Crystal Chemistry of Uranium Tellurides

III. Temperature-Dependent Structural Investigations on Uranium Ditelluride

K. Stöwe

Institut für Anorganische und Analytische Chemie und Radiochemie, Universität des Saarlandes, D-66041 Saarbrücken, Germany

Received April 8, 1996; in revised form August 19, 1996; accepted August 26, 1996

Single crystals of the title compound up to a size of 5 mm were available from the elements via chemical transport reactions with $TeBr_4$ as transporting agent. The analysis by atomic emission spectrometry gave $UTe_{1.99(5)}$, i.e., stoichiometric composition. By single-crystal structure analysis we confirmed earlier results, according to which UTe_2 crystallizes orthorhombic in a unique structure type [space group *Immm*, $Z = 4$ with $a = 416.22(3)$ pm, $b = 613.29(4)$ pm, and $c = 1397.1(1)$ pm at ambient temperature]. The structure is built up by bicapped trigonal prisms of tellurium, connected via faces to fourfold capped biprisms. Because of the side-by-side arrangement pattern of the biprisms, linear chains of telluriums with distances far shorter than the nonbonding distance of Te^{2-} ions and slight alternation are observed. We report the results of an elaborate refinement of the crystal structure determined by X-ray diffraction ($R_w = 1.72\%$) and their behavior in the temperature range $10\ K < T < 573\ K$ using both powdered and single-crystalline samples to detect phase transitions as indications of structural or electronic changes.

INTRODUCTION

In the phase diagram of the system U/Te (1) the binary compound UTe_2 is found at the border line between the polytelluric compounds of higher tellurium content, e.g., UTe_3 and UTe_5, and the ''reduced'' tellurides of lower content, e.g., UTe, U_2Te_3, U_3Te_4, and U_7Te_{12}. At first sight U^{4+} and Te^{2-} ions are to be expected for UTe_2 in the stoichiometric relation of 1:2, but looking at the crystal structure short Te–Te distances far below the sum of the radii of Te^{2-} ions attract one's attention immediately. These tellurium ions form linear chains with alternating homonuclear distances. The only compound known so far with equidistant chains of Te and semimetallic behavior is TlTe (2). Below 170 K TlTe shows a phase transition (3) and it is speculated that this transition leads to a Peierls distortion of the tellurium chain (4). In the case of UTe_2 the alternation is not very pronounced, the difference between bond lengths being only about 2 pm, and one might expect both, further differentiation of distances on cooling and equalization on heating. So we intended to perform X-ray structural investigations at varying temperatures. In addition to powder investigations we performed single-crystal examinations down to temperatures as low as possible, because the expected structural changes would not necessarily lead to a drastic change in the powder pattern. To determine whether UTe_2 is already distorted in the sense given above and whether the distortion increases on cooling, we looked for other U/Te compounds with linear Te chains. A promising candidate was α-UTe_3 in the $ZrSe_3$ structure type, but as structural data from single-crystal investigations were lacking, we first had to grow single crystals (5). In the course of this work we were able to confirm the existence of the compound U_2Te_5, that was proposed in the literature and that crystallizes in a new structure type with linear Te chains too (6).

Another feature of the UTe_2 structure merits attention. Because of face sharing of two cation-coordination polyhedra we find a single short U–U distance, comparable to those in compounds such as US and UO_2. From photoelectron spectroscopy (PES) it is known that the *f* electrons are delocalized in US. UTe_2 is unique insofar as there is only one short distance in this compound, whereas in US having a NaCl-type structure a three-dimensional arrangement of homonuclear interactions is observed as in all other metallic uranium compounds. In view of this possible interaction and together with the observation of polyanionic structure fragments the question of the oxidation state of uranium in this compound is especially interesting.

SAMPLE SYNTHESIS

The uranium tellurides investigated were prepared as black, lustrous crystals up to a size of 5 mm by chemical transport reactions in evacuated and sealed silica ampoules with $TeBr_4$ as transporting agent. $TeBr_4$ was synthesized from the elements and purified by sublimation. Starting materials for the uranium tellurides were stoichiometric

0022-4596/96 $18.00

amounts of the elements, i.e., uranium (99.9% purity, Kelpin, Leimen, Germany) cut from a block and pieces of tellurium (99.999%, Fluka). The temperature gradient for transport was 950 to 850°C. As the products are air and moisture sensitive, they were handled under a dry and oxygen-free atmosphere of argon in a glove box. For purposes of characterization the products were analyzed by inductively coupled plasma atomic emission spectrometry (ICP-AES) and X-ray diffraction methods. Further details can be found in (5).

EXPERIMENTAL

Powdered samples of uranium ditelluride were investigated with a variable-temperature Guinier diffractometer Model 645 (Huber, Germany) with a scintillation counter and a Ge(220) crystal monochromator at a Cu X-ray source ($CuK\alpha_1$) operating in transmission geometry. Low temperatures down to 10 K were achieved by a two-stage helium Cryodyne Refrigeration System (CTI Cyrogenics, USA), a Model SC Compressor, and a Model 22 Cold Head, mounted with its second stage at the sample chamber. For temperatures above 10 K the second stage of the cold head was surrounded by a heating wire, and the heating power was adjusted with a Model DRC-81C PID-controller (Lake Shore Cryotronics, Inc., USA) with a Si diode as temperature sensor, mounted directly at the sample holder. The temperature stability during the ~45-h data collection was better than ±0.1 K. The temperature scale was calibrated with the temperatures of well-known polymorphic phase transitions. The goniometer was adjusted using the procedure proposed in (7). During the measurement the sample chamber was evacuated ($<10^{-3}$ mbar). Temperature setting, step motor control, and data readout were achieved with the IEEE-488 bus of the temperature controller connected to an IBM-compatible PC. A stepwidth of $0.01°2\theta$ and a counting time of 20 s per step were set by the control software. After a temperature change the sample was equilibrated for more than 48 h before a new measurement was started. Subsequently the diffraction data were analyzed using a full-profile Rietveld program (8). Silicon (99.999%, Johnson Matthey) was used as external standard (a = 543.088 pm, JCPDS File No. 27-1402). The results are summarized in Table 1. Further discussion of the positional parameters of the individual atoms did not seem advisable because of strong absorption and texture effects.

The lattice parameters can be compared with those from the X-ray single-crystal structure analysis in the temperature interval from about 120 to 290 K. The data collections were carried out with a P4 single-crystal diffractometer (Siemens, Karlsruhe, Germany), and the structure refinement with the program SHELXTL (9). For low-temperature measurements the diffractometer was equipped with a Siemens LT-2A Low Temperature Attachment using a Watlow Series 985 temperature controller. Precision and long-time stability of the sample temperature were better than ±1 K. The temperature values were calibrated after the data collections separately with a coated Ni/Cr–Ni thermocouple (Type K, Conatex, St. Wendel, Germany) placed at the crystal position. Above ambient temperature a heatable goniometer head Type FR 559 (Enraf-Nonius, Delft, The Netherlands) with a Ni/Cr–Ni thermocouple (Type K) was used. Precision and stability of this instrument were better than ±2 K during measurement. Tables 2 to 4 summarize important measurement and refinement data including the refined parameters and Table 5 gives selected interatomic distances below 500 pm. To confirm the stoichiometric composition of UTe_2 produced by transport reactions, chemical analysis were performed by ICP-AES. This gave an averaged chemical formula of $UTe_{1.99(5)}$.

TABLE 1

Results of the Rietveld Refinement in the Temperature Interval 297–10 K with Reference to Silicon as Standard (a = 543.088 pm, JCPDS File No. 27-1402)[a]

Temperature (K)	a (pm)	b (pm)	c (pm)
297	416.37(1)	612.36(2)	1395.47(4)
267	416.09(1)	611.93(2)	1394.58(4)
237	415.88(1)	611.60(2)	1393.83(4)
207	415.59(1)	611.39(2)	1392.90(4)
199	415.46(1)	611.40(1)	1392.88(4)
169	415.39(1)	611.19(1)	1392.58(3)
139	415.21(1)	611.07(2)	1392.06(4)
119	415.22(1)	611.15(2)	1392.44(4)
110	415.15(1)	611.19(1)	1392.19(4)
100	414.99(1)	611.14(1)	1391.93(4)
96	414.90(1)	610.76(2)	1391.34(4)
92	414.68(1)	610.49(1)	1390.69(4)
62	414.67(1)	610.58(2)	1391.02(4)
32	414.56(1)	610.58(1)	1390.89(4)
[10	414.70(1)	610.66(1)	1390.83(5)]

[a] At 10 K the compound is already in a metastable form (symbolized by brackets).

CRYSTAL STRUCTURE

The crystal structure of uranium ditelluride has been controversial for a time (10, 11). By X-ray single-crystal structure analysis Beck and Dausch (12) were able to confirm the model proposed by Klein Haneveld and Jellinek (13) from powder methods. In this work this model is further confirmed and additionally the structure refinement data are improved.

In the orthorhombic body-centered cell of uranium ditelluride we find one crystallographically independent uranium site with symmetry $mm2$. The uranium ions are sur-

TABLE 2
Measurement Data for Uranium Ditelluride in the X-Ray Single-Crystal Structure Analysis[a]

Chemical formula	UTe_2
Molecular weight	493.2 g mol^{-1}
Crystal size	0.11 × 0.07 × 0.12 mm (LT) 0.26 × 0.19 × 0.14 mm (HT)
Color	Lustrous black
Number of formula units per cell	4
Space group	*Immm* (No. 71)
Diffractometer type	Siemens P4 with XSCANS (21)
Measured range of reciprocal space (Mo$K\alpha$)	$3° < 2\theta < 70°$ (*hkl*, *hkl*, *hkl*, *hkl*) (LT) $3° < 2\theta < 60°$ (all octants) (HT)
Monochromator	Plan HOPG crystal
Scan type	ω-2θ
Scan range	0.7°θ in 96 steps
Scan speed	Variable, 2–10.2° min^{-1}
Absorption correction	Numerical
Structure solution	Direct methods
Structure refinement	Full matrix least-squares
Program for solution and refinement	SHELXTL PLUS (9)
Extinction parameter	Empirical with $F^* = F[1 + 0.002\,\chi F^2/\sin(2\theta)]^{-1/4}$
Number of independent parameters	14

[a] LT, low-temperature; HT, high-temperature data collection.

rounded by eight tellurium ions from two different lattice sites, Te(1) and Te(2), in the form of a bicapped trigonal prism (see Fig. 1). Two such coordination polyhedra share the third uncapped face, consisting of four Te(2) ions, to form fourfold capped biprisms as building units with a U–U distance of 377.9(1) pm at room temperature. In the [100] direction the biprisms share triangular faces and they are stacked to infinite chains in the periodicity of the *a* translation. In the [010] direction these biprism chains lie side by side in the periodicity of the *b* translation without being connected via common ions. In this direction we find exact linear chains of Te(2) ions with slightly alternating distances [305.7(1) pm within one biprism and 307.6(1) pm between them, see Fig. 2]. In the third direction, [001], the biprism chains are stacked in the fashion of a body-centered lattice. Polyhedra chains of fourfold capped biprisms are also found in metallic $NbAs_2$ (14), but with a topologically different connectivity pattern ($Nb^{5+}As^{3-}As^{2-}$ with $[As_2]^{4-}$ dumbbells connecting the biprism chains).

Comparison of the Te(2)–Te(2) distances with the distance for a covalent single bond [271 pm in diphenylditelluride (15)] on the one side and a nonbonding distance on the other side [twice the ionic radius of a Te^{2-} ion: 442 pm in CN 6 (16)] gives a broken bond order. In contrast, the shortest interatomic distances of the Te(1) ions to other tellurium ions [383.1(1) pm at room temperature] indicate

TABLE 3
Refinement Data for Uranium Ditelluride as a Function of Temperature in the X-Ray Single-Crystal Structure Analysis

Temperature (K)	293	230	215	200	185	169	138	118
Lattice parameters (pm)								
a	416.22(3)	415.70(3)	415.60(3)	415.50(4)	415.40(3)	415.34(4)	415.10(4)	415.12(3)
b	613.29(4)	612.57(5)	612.51(5)	612.38(5)	612.30(5)	612.10(6)	611.98(7)	611.98(6)
c	1397.1(1)	1395.7(1)	1395.4(1)	1395.0(1)	1394.7(1)	1394.4(1)	1393.6(1)	1393.7(1)
Calculated density (g cm^{-3})	9.186	9.218	9.223	9.230	9.235	9.242	9.254	9.253
Linear absorption coefficient (mm^{-1})	61.26	61.47	61.51	61.55	61.59	61.64	61.71	61.59
No. of observed reflections	1842	1685	1864	1720	1790	1815	1813	1729
No. of nonequivalent reflections	480	452	480	456	480	480	480	458
Internal *R* value	0.0320	0.0494	0.0348	0.0496	0.0373	0.0485	0.0467	0.0413
Extinction parameter	0.0041(1)	0.0043(1)	0.0043(1)	0.0043(1)	0.0044(1)	0.0043(1)	0.0045(1)	0.0045(1)
R value	0.0214	0.0285	0.0198	0.0288	0.0274	0.0290	0.0289	0.0274
R_w value [$w = 1/\sigma(F_o)^2$]	0.0172	0.0202	0.0160	0.0198	0.0195	0.0183	0.0187	0.0199
Temperature (K)	293	333	393	453	513	573		
Lattice parameters (pm)								
a	415.48(5)	415.71(5)	416.21(4)	416.64(5)	417.10(5)	417.57(6)		
b	612.65(6)	613.04(5)	613.50(5)	614.05(6)	614.60(6)	615.07(7)		
c	1395.7(2)	1396.6(2)	1397.9(2)	1399.5(2)	1400.5(2)	1402.0(2)		
Calculated density (g cm^{-3})	9.222	9.205	9.178	9.150	9.125	9.098		
Linear absorption coefficient (mm^{-1})	61.38	61.39	61.21	61.04	60.85	60.67		
No. of observed reflections	1844	1959	1972	1983	1983	1984		
No. of nonequivalent reflections	475	315	318	319	320	320		
Internal *R* value	0.0319	0.0481	0.0478	0.0477	0.0516	0.0452		
Extinction parameter	0.0054(2)	0.0058(2)	0.0059(2)	0.0056(2)	0.0051(3)	0.0014(1)		
R value	0.0366	0.0318	0.0305	0.0291	0.0336	0.0294		
R_w value [$w = 1/\sigma(F_o)^2$]	0.0251	0.0236	0.0216	0.0213	0.0268	0.0251		

TABLE 4
Positional Parameters and Temperature Factors of the Compound UTe_2 as a Function of Temperature[a]

	Atom	Wyckoff letter	Symmetry	Position
	U	4*i*	*mm*2	0 0 *z*
	Te(1)	4*j*	*mm*2	$\frac{1}{2}$ 0 *z*
	Te(2)	4*h*	*m*2*m*	0 *y* $\frac{1}{2}$

Temperature (K)	293	230	215	200	185	169	138	118
U								
z	0.13523(2)	0.13511(2)	0.13509(1)	0.13509(2)	0.13510(2)	0.13505(2)	0.13502(2)	0.13500(2)
U_{11}	78(1)	69(1)	60(1)	60(1)	60(1)	52(1)	47(1)	52(1)
U_{22}	90(1)	83(2)	68(1)	73(2)	68(2)	65(2)	52(2)	52(2)
U_{33}	78(1)	68(1)	59(1)	60(1)	55(1)	53(1)	45(1)	42(1)
Te(1)								
z	0.29779(3)	0.29788(4)	0.29796(3)	0.29794(3)	0.29797(3)	0.29793(3)	0.29802(3)	0.29806(3)
U_{11}	96(2)	84(2)	75(1)	72(2)	70(2)	63(2)	55(2)	56(2)
U_{22}	83(2)	77(3)	62(2)	67(3)	63(3)	57(2)	49(3)	50(2)
U_{33}	84(2)	71(2)	65(1)	63(2)	59(2)	55(2)	48(2)	43(2)
Te(2)								
y	0.2508(1)	0.2508(1)	0.2508(1)	0.2509(1)	0.2508(1)	0.2507(1)	0.2507(1)	0.2508(1)
U_{11}	85(2)	75(2)	68(1)	66(2)	65(2)	55(2)	51(3)	50(2)
U_{22}	79(2)	73(3)	59(2)	65(3)	56(3)	56(2)	48(3)	48(3)
U_{33}	90(2)	76(2)	67(1)	65(2)	63(2)	58(2)	50(2)	46(2)

Temperature (K)	293	333	393	453	513	573
U						
z	0.13520(2)	0.13530(2)	0.13536(2)	0.13544(2)	0.13550(3)	0.13560(2)
U_{11}	73(1)	101(2)	116(2)	132(2)	170(3)	157(3)
U_{22}	84(2)	124(2)	141(2)	158(2)	180(3)	182(3)
U_{33}	67(2)	83(3)	101(2)	113(2)	127(3)	144(2)
Te(1)						
z	0.29780(5)	0.29779(5)	0.29774(4)	0.29765(4)	0.29761(5)	0.29750(5)
U_{11}	96(2)	124(3)	142(2)	159(2)	205(3)	193(4)
U_{22}	81(2)	118(3)	133(3)	150(3)	171(4)	168(4)
U_{33}	75(2)	86(2)	106(3)	118(3)	132(4)	154(3)
Te(2)						
y	0.2508(1)	0.2509(1)	0.2510(1)	0.2509(1)	0.2510(1)	0.2509(1)
U_{11}	85(2)	115(2)	129(3)	146(3)	188(4)	176(4)
U_{22}	76(2)	108(3)	126(3)	138(3)	159(4)	155(4)
U_{33}	79(2)	86(2)	108(4)	122(4)	138(5)	167(3)

[a] U_{ij} values are given in pm^2. $U_{12} = U_{13} = U_{23} = 0$. The dimensions are in accordance with the following formula: $-2\pi^2 \sum_i \sum_j U_{ij} h_i h_j a_i^* a_j^*$.

no homonuclear covalent interactions. To describe the compound within the Zintl–Klemm concept one would give the formula $U^{3+}Te^{2-}\,{}^1_\infty[Te^-]$, assuming integral oxidation states and a bond order of 0.5 between the Te(2) ions in the linear chains and neglecting that the distances between the Te(2) ions are slightly alternating.

The short U–U distance poses the question whether there is a homonuclear interaction between the uranium ions. Comparing its value [377.9(1) pm] with the sum of ionic radii [$r(U^{3+})$[8] = 111 pm taken from UI_3 (17)], this seems at first sight unreasonable; however, it is already known that the 5*f* wavefunctions extend much more in space than the 4*f* wavefunctions, so that bond formation with the contribution of *f* orbitals may be discussed (18, 19). Localized *f* states were found by photo emission spectroscopy (20) in UO_2 [*d*(U–U) = 386.7 pm], whereas in US [*d*(U–U) = 387.8 pm] a narrow *f* band was observed. So in UTe_2, too, an *f* overlap cannot be ruled out.

DISCUSSION OF CHANGES IN THE STRUCTURAL PARAMETERS AS A FUNCTION OF TEMPERATURE

A. Single-Crystal Investigations

Figure 3 gives the relative changes of the lattice parameters of the orthorhombic cell as derived from the single-crystal investigations (Table 3) as a function of temperature in the interval 118 to 573 K. There are neither discontinuities nor plateaus, which would be indications of changes in the structure. The thermal contraction is almost equal in all three lattice directions. Contraction in the [010] direction, i.e., along the Te(2) chains, shows the smallest variation with temperature. From the single-crystal data re-

TABLE 5
Selected Interatomic Distances in UTe_2 below 500 pm (in pm)

Temperature (K)	293	230	215	200	185	169	138	118
U–Te coordination polyhedra								
U–Te(1) prism 2×	308.05(4)	307.90(5)	307.94(4)	307.83(5)	307.80(4)	307.75(4)	307.70(4)	307.78(4)
U–Te(2) prism 4×	319.94(3)	319.49(4)	319.39(2)	319.29(4)	319.26(3)	319.19(4)	318.99(3)	318.98(3)
U–Te(1) cap 2×	320.61(2)	320.24(3)	320.19(3)	320.13(3)	320.07(3)	320.00(3)	319.90(4)	319.90(3)
Mean U–Te distance	317.14(5)	316.78(7)	316.73(5)	316.64(7)	316.60(6)	316.53(6)	316.40(6)	316.41(5)
U–U distances								
U–U in the biprisms	377.87(6)	377.17(6)	377.00(4)	376.90(6)	376.86(6)	376.62(7)	376.33(7)	376.30(6)
U–U in chain of biprisms	416.22(3)	415.70(3)	415.60(3)	415.50(4)	415.40(3)	415.34(4)	415.10(4)	415.12(3)
Te–Te distances								
Te(1)–Te(2) cap to prism	383.13(4)	382.59(5)	382.43(4)	382.39(5)	382.26(4)	382.17(4)	381.90(4)	381.90(4)
Te(1)–Te(1) cap to prism	393.92(3)	393.54(4)	393.56(4)	393.44(4)	393.41(4)	393.27(4)	393.22(4)	393.26(4)
Te(1)–Te(1) in prism	416.22(3)	415.70(3)	415.60(3)	415.50(4)	415.40(3)	415.34(3)	415.10(4)	415.12(3)
Te(1)–Te(2) in prism	443.23(5)	442.90(6)	442.89(5)	442.72(6)	442.71(5)	442.58(6)	442.45(6)	442.52(6)
Te(2)–Te(2) in prism	305.7(1)	305.4(1)	305.3(1)	305.1(1)	305.2(1)	305.2(1)	305.1(1)	305.0(1)
Te(2)–Te(2) prism–prism	307.6(1)	307.2(1)	307.2(1)	307.3(1)	307.1(1)	306.9(1)	306.9(1)	306.9(1)
Te(2)–Te(2) in prism	416.22(3)	415.70(3)	415.60(3)	415.50(4)	415.40(3)	415.34(4)	415.10(4)	415.12(3)

Temperature (K)	293	333	393	453	513	573
U–Te coordination polyhedra						
U–Te(1) prism 2×	307.66(6)	307.74(6)	307.95(5)	308.10(5)	308.28(7)	308.40(6)
U–Te(2) prism 4×	319.47(4)	319.75(4)	320.09(4)	320.49(4)	320.80(5)	321.25(5)
U–Te(1) cap 2×	320.28(4)	320.45(3)	320.69(3)	320.99(3)	321.26(4)	321.52(4)
Mean U–Te distance	316.7(1)	316.9(1)	317.2(1)	317.5(1)	317.8(1)	318.1(1)
U–U distances						
U–U in the biprisms	377.39(7)	377.93(7)	378.44(7)	379.08(7)	379.5(1)	380.22(8)
U–U in chain of biprisms	415.48(5)	415.71(5)	416.21(4)	416.64(5)	417.10(5)	417.57(6)
Te–Te distances						
Te(1)–Te(2) cap to prism	382.64(6)	382.90(6)	383.35(5)	383.83(5)	384.24(7)	384.72(7)
Te(1)–Te(1) cap to prism	393.44(5)	393.67(5)	393.98(4)	394.27(5)	394.60(5)	394.85(6)
Te(1)–Te(1) in prism	415.48(5)	415.71(5)	416.21(4)	416.64(5)	417.10(5)	417.57(6)
Te(1)–Te(2) in prism	442.78(8)	443.06(8)	443.37(7)	443.74(7)	444.0(1)	444.3(1)
Te(2)–Te(2) in prism	305.3(1)	305.5(1)	305.6(1)	305.9(1)	306.0(2)	306.4(1)
Te(2)–Te(2) prism–prism	307.4(1)	307.6(1)	307.9(1)	308.2(1)	308.6(2)	308.7(1)
Te(2)–Te(2) in prism	415.48(5)	415.71(5)	416.21(4)	416.64(5)	417.10(5)	417.57(6)

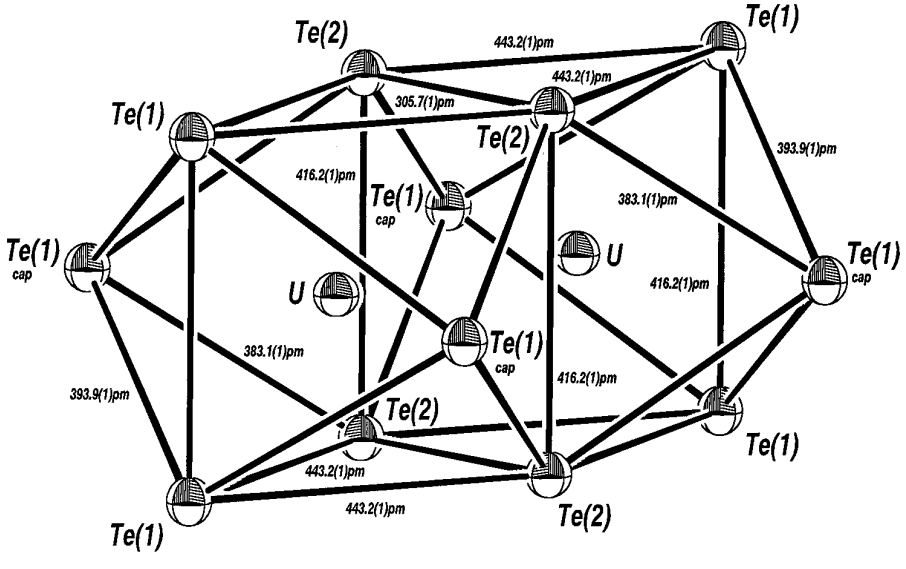

FIG. 1. Coordination polyhedra around the U ions in UTe_2 [distances (pm) at room temperature].

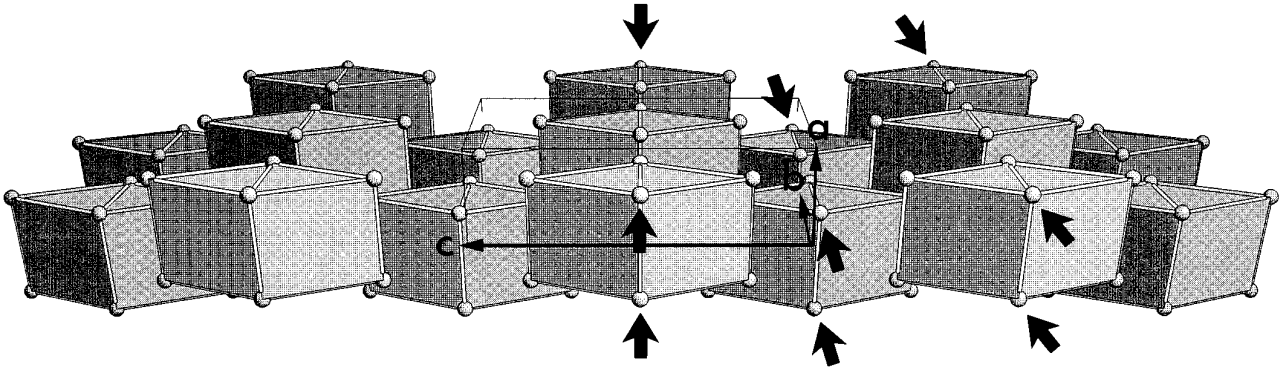

FIG. 2. Crystal structure of UTe_2 in a [010] projection (tilted by ≈30°). For simplification the prism caps were omitted. Linear Te(2) chains are emphasized by arrows.

finement of the structural parameters the positional coordinates of the three atom types of Table 4 are graphically represented in Fig. 4. While y(Te(2)) slightly decreases with decreasing temperature, z(Te(1)) increases in contrast to z(U), which decreases too. In the end the contraction of the lattice parameters and the increase in z(Te(1)) compensate each other, so that the U–Te(1) distance remains almost constant (see Fig. 5); however, the U–U distance is considerably reduced at lower temperatures and this is quite remarkable. According to Pauling's rules, cation–cation distances reduce in coordination polyhedra sharing common faces only for covalent interactions, whereas anion–anion distances of the common face enlarge. A reduction of z(U) should be accompanied by an increase in the area of the common face, i.e., an enlargement the Te(2)–Te(2) distances within the polyhedron, equivalent to a reduction in the alternation of distances within the Te(2) chain. A direct measure for the alternation is the y parameter of Te(2). As seen from Fig. 4, in fact, a reduction is observed.

B. Powder Investigations

The limit of the LT2 low temperature device for the P4 single-crystal diffractometer is reached at about 115 K.

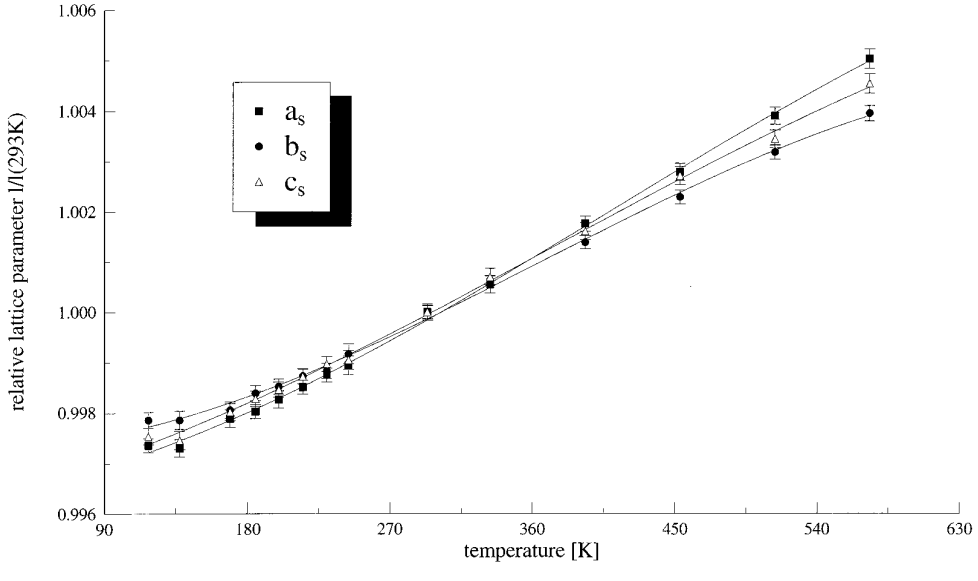

FIG. 3. Relative changes in the lattice parameters of UTe_2 from the single-crystal investigations as a function of temperature in the interval 118 to 573 K.

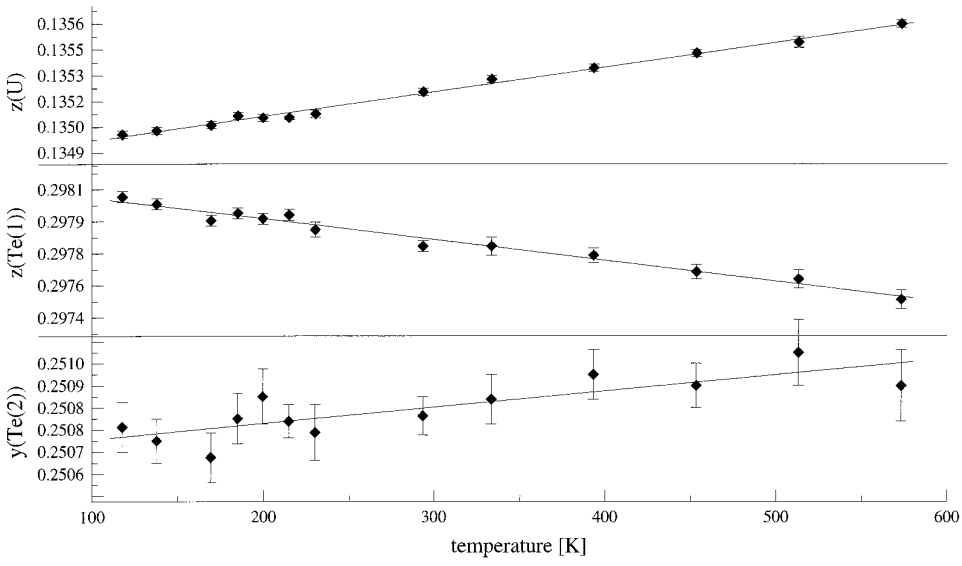

FIG. 4. Changes in the positional parameters z(U), z(Te(1)), and y(Te(2)) of UTe_2 as a function of temperature of the single-crystal investigations.

Below this temperature only investigations on powdered samples by the Guinier diffractometer with helium refrigerator had been possible up to now. Figure 6 summarizes the results from the full-profile Rietveld refinement (filled symbols). In the temperature region between 119 K and room temperature, the dilatometric behavior is in good agreement with the data from single-crystal investigations (open symbols). Between 92 and 110 K a sudden change in the lattice parameters is observed. At 100 K the *a* axis length begins to decrease continuously first; the lengths of the other two axes, *b* and *c*, follow at 96 K. Below 92 K the unit cell parameters remain nearly constant. The relative shrinkage of the lattice parameters is almost uniform in the three directions. Since the phase transformation is not accompanied by a symmetry change detectable with powder methods and since no systematic changes in the positional parameters of the atoms derived from the Rietveld refinements could be seen because of their errors, we are

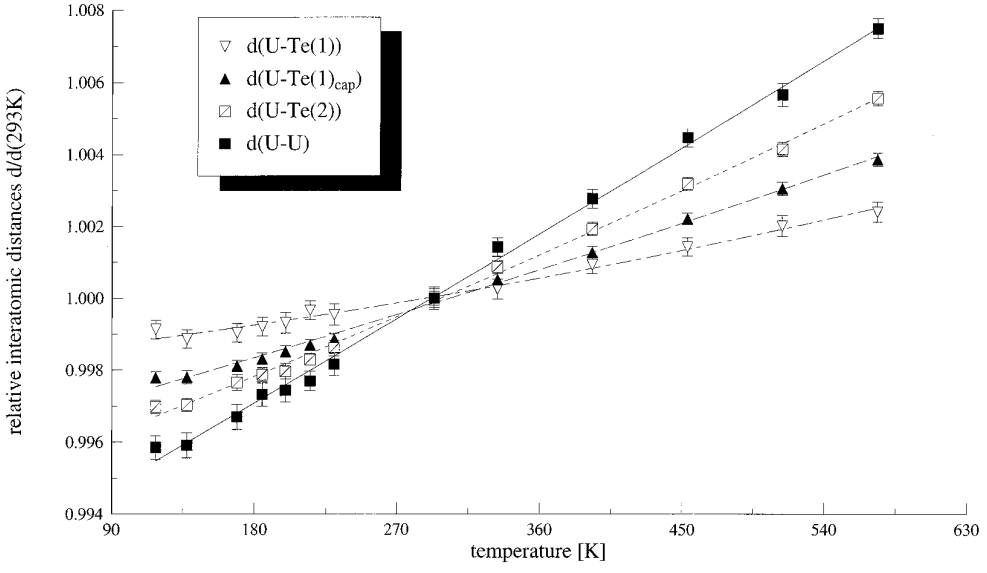

FIG. 5. Relative changes in interatomic distances in UTe_2 as a function of temperature of the single-crystal investigations.

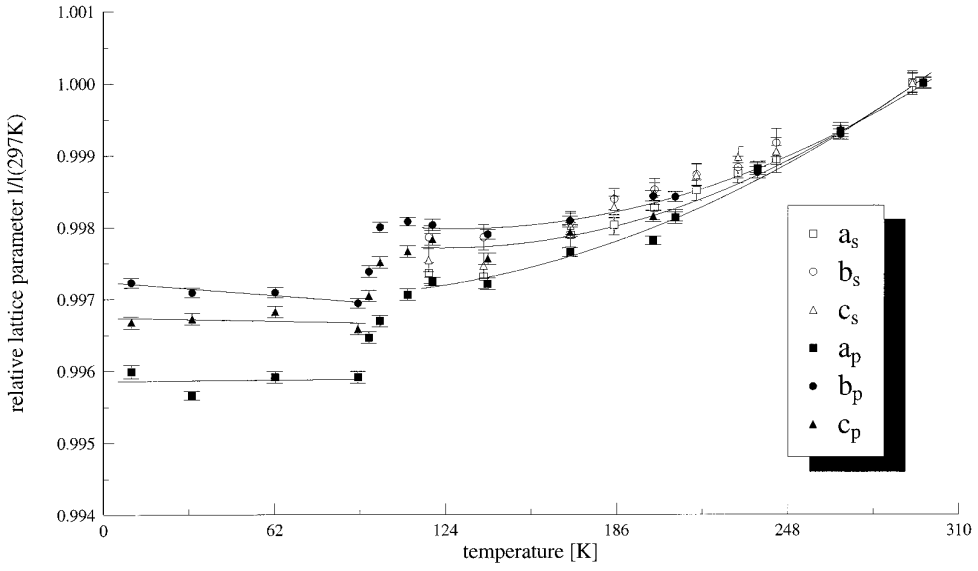

FIG. 6. Relative changes in the lattice parameters of UTe_2 from powder investigations (filled symbols) as a function of temperature in the interval between 10 and 297 K. For the purpose of comparison, single-crystal data from Fig. 3 (open symbols) were added.

not able to give a statement about the nature of the transition.

Below 23 K new reflections appeared after long cooling times. The transformation of UTe_2 at these temperatures is very sluggish and is not completed even after 100 days. From the diffraction pattern of the low-temperature phase no isotypic relation to other AX_2 phases of known structure type is observed. Accordingly, the structure and stoichiometry of the new phase remain unknown. The transformation is reversible and proceeds within minutes on warming up. We are currently preparing for high-pressure experiments hoping to detect a similar transformation at ambient temperatures.

Common features of the uranium tellurides UTe_2, U_2Te_5, and UTe_3 are linear Te chains with alternating distances as structural fragments. From a topological view the transition from a chain of equidistant telluriums to one with alternating distances is similar to a Peierls distortion usually found in compounds with cation chains, and the question arises whether tellurium chains behave electronically analogous too. From X-ray investigations of the uranium polytellurides we learn that in these systems different degrees of alternation can be realized; however, in the compound UTe_2 the Te chains remain roughly equidistant. In the temperature-dependent X-ray powder investigations, indications for phase transitions were found; however, the nature of the transformations remains hitherto unknown. In the compound UTe_3 the alternation shows another extreme: a distance typical for a single covalent Te bond alternates with a much larger value and this feature would explain the semiconducting properties of the compound. By comparison with $ZrTe_3$ the borderline between semimetallic and semiconducting properties can be limited to the distance interval from 310 pm ($ZrTe_3$) to 335 pm (UTe_3). From this we would expect a semimetallic character for UTe_2 and U_2Te_5 too. We are currently preparing experiments to measure the conductivity of the aforementioned compounds.

REFERENCES

1. V. K. Slovyanskikh, E. I. Yarembash, G. V. Ellert, and A. A. Eliseev, *Izv. Akad. Nauk SSSR Ser. Khim. Neorg. Mater.* **4,** 543 (1968).
2. A. A. Toure, G. Kra, R. Eholie, J. Olivier-Fourcade, and J.-C. Jumas, *J. Solid State Chem.* **87,** 229 (1990).
3. J. D. Jensen, J. R. Burke, D. W. Ernst, and R. Allgaier, *Phys. Rev. B* **6,** 319 (1972).
4. W. H. E. Schwarz, DFG-communication, Siegen, 1992.
5. K. Stöwe, *Z. Anorg. Allg. Chem.* **622,** 1419 (1996).
6. K. Stöwe, *Z. Anorg. Allg. Chem.* **622,** 1423 (1996).
7. J. J. Fitzpatrick and J. S. Presnall, *Adv. X-Ray Anal.* **27,** 313 (1984).
8. "WYRIET, Version 3: Powder Profile Refinement and Structure Analysis Package for Personal Computers," M. Schneider, Pöcking, Germany.
9. "SHELXTL PLUS, Version 4.0: Program for Determination of Crystal Structures with X-ray and Neutron Data." Siemens Analytical X-Ray Instruments, Inc., Madison, WI, 1990.
10. A. J. Klein Haneveld and F. Jellinek, *J. Less-Common Met.* **19,** 123 (1969).
11. F. Ferro, *Z. Anorg. Allg. Chem.* **275,** 320 (1954).
12. H. P. Beck and W. Dausch, *Z. Naturforsch. B* **43,** 1547 (1988).
13. A. J. Klein Haneveld and F. Jellinek, *J. Less-Common Met.* **21,** 45 (1970).
14. S. Furuseth and A. Kjekshus, *Acta Crystallogr.* **18,** 320 (1965).

15. G. Llabres and O. Dideberg, *Acta Crystallogr. B* **28,** 2438 (1972).
16. R. D. Shannon, *Acta Crystallogr. A* **32,** 751 (1976).
17. J. H. Levy, J. C. Taylor, and P. W. Wilson, *Acta Crystallogr. B* **31,** 880 (1975).
18. J. M. Fournier, *in* ''Actinides: Chemistry and Physical Properties'' (L. Manes, Ed.), p. 132. Springer, Berlin, 1985.
19. H. H. Hill, ''Plutonium 1970'' (W. M. Miner, Ed.), p. 2. Met. Soc. AIME, New York, 1970.
20. J. M. Fournier and L. Manes, *in* ''Actinides: Chemistry and Physical Properties'' (L. Manes, Ed.), p. 51. Springer, Berlin, 1985.
21. ''XSCANS, Version 2.1: X-Ray Single Crystal Analysis Software.'' Siemens Analytical X-Ray Instruments, Inc., Madison, WI, 1994.